# Dalton Transactions

Accepted Manuscript






ROYAL SOCIETY OF CHEMISTRY

www.rsc.org/dalton

# Structure Refinement and Photocatalytic Properties of Porous POMCPs by Selecting the Isomerous PYTTZ

Liang Li [a,b], Jing-Wen Sun[a], Jing-Quan Sha[a* b], Guang-Ming Li[a], Peng-Fei Yan[a*], Cheng Wang[a], Lian Yu [b]

[a]*Key Laboratory of Functional Inorganic Material Chemistry (MOE), P. R. China; School of Chemistry and Materials Science, Heilongjiang University; Harbin 150080, P. R. China*

[b]*The Key Laboratory of Biological Medicine Formulation，Heilongjiang Provincial; School of Pharmacy, Jiamusi University, Jiamusi, 154007, PR China*

**Abstract:** Two polyoxometalates based coordination polymers (POMCPs) constructed form Keggin POMs and $Ag^{+}$ with pyttz were synthesized, $[Ag_4(H_2pyttz\text{-}I)(H_2pyttz\text{-}II)(Hpyttz\text{-}II)][HSiW_{12}O_{40}]\cdot 4H_2O$ (**1**) and $[Ag_4(H_2pyttz\text{-}II)(Hpyttz\text{-}II)_2][H_2SiW_{12}O_{40}]\cdot 3H_2O$ (**2**). ($H_2$pyttz-I = 3-(pyrid-2-yl)-5-(1H-1,2,4-triazol-3-yl)-1,2,4-triazolyl; $H_2$pyttz-II = 3-(pyrid-4-yl)-5-(1H-1,2,4-triazol-3-yl)-1,2,4-triazolyl). Both compounds have the similar building units, the similar stick-like units and the similar 1D inorganic chains, but finally obtain the different motifs of tunnels (tunnel A in **1** and tunnel A&B in **2**). By careful inspection of structures of **1** and **2**, it is believed that the isomerous pyttz molecules can precisely refine the structure of porous POMCPs without changing the underlying framework, which is favor of the study about the structure-activity relationship of POMCPs. Furthermore, the results of the photocatalytic activities show that compound **2** exhibits higher photocatalytic activity than that of compound **1**, which is consistent with their structural characteration.

**Keywords**: Polyoxometalates. Porous POMCPs. Photocatalytic activity. Structure-activity relationship

## Introduction

The achievement of effective catalysis, adsorption and ion exchanges in porous materials requires the careful design of their structures, particularly the shape of the guest-accessible space and the chemical interaction of guest and pore surfaces. In this respect, porous coordination polymers (PCPs) [1] have spurred increasing interest in extending the range of framework topologies and chemical compositions. [2] Polyoxometalates (POMs), as one kind of important metal oxide cluster with nanosizes, abundant topologies, and great potential applications in catalysis, magnetism, materials science,[3] have been employed as secondary building units (SBUs) to construction of organic-inorganic hybrid materials,[4] in particular, to be introduced into the CPs for the construction of multifunctional POM-based coordination polymers (POMCPs). [5]

Recently, numerous crystalline PCPs have been constructed and their porosity has been exploited for a variety of applications.[6] More significantly, various of strategies have been shown in constructing the diverse multi-functional porous materials (Table S1).[7-10] For example, Joanne I. Yeh et al. has successfully constructed a porous metal-organic framework (MOF) (Bio-MOF-100) *via* rational design of the size of the vertex with lowest crystal density (0.302 $g.cm^{-3}$) and the largest MOF pore volume (4.3 $cm^3.g^{-1}$). [7] Bu X. H. et al. revealed the strategy for encapsulating both single metal ions and dimeric or trimeric clusters into MOFs, in order to enhance the photocatalytic activity for decomposition of methyl orange.[11] In comparison with PCPs, the rational design and assembly of porous POMCPs are more challengeable and lots of synthesis strategies become unreliably due to the nature of POMs. On one hand, POMs exhibit a wide variety of structural motifs with different sizes and topologies, ranging from closed cages and spherical shells to basket–, bowl–, barrel– and belt–shaped structures.[12] On the other hand, POMs possess a large number of oxygen atoms as potential active coordination sets to combine with CPs, and the number and mode of combined CPs is often uncertain. Therefore, when POMs are used as SBUs, it is difficult to predict the primary self-assembly style in contrast with CPs. More importantly, when the structure of materials is adjusted, the underlying framework remains intact, which is favor of the study of the structure-activity relationship. So controlling and regulating the fine structures of POMCPs will become a great hot spot.

The synthesis progress about porous POMCPs has been made on the practical manipulation by our group,[13] and the tunnel motifs of POMCPs could be regulated by choosing different $H_2$pyttz molecules. It is regret that the underlying framework was also changed, when the motifs of POMCPs were regulated.[14] Based on the previous work and comprehensive consideration, and to obtain and control the tunnel motifs of POMCPs, we rely on the suitably designed structure and coordination mode of organic molecules as a general strategy for the preparation of target compounds. Herein, we select pyttz-I and pyttz-II (Scheme S1) to connect with POMs and silver atoms to construct POMCPs with the similar underlying framework. Fortunately, compounds **1** and **2** are isolated successfully and exhibit the similar structure and the different tunnels (Scheme 1). Furthermore, we also investigated their photocatalytic activities about the decomposition of Rhodamine B.

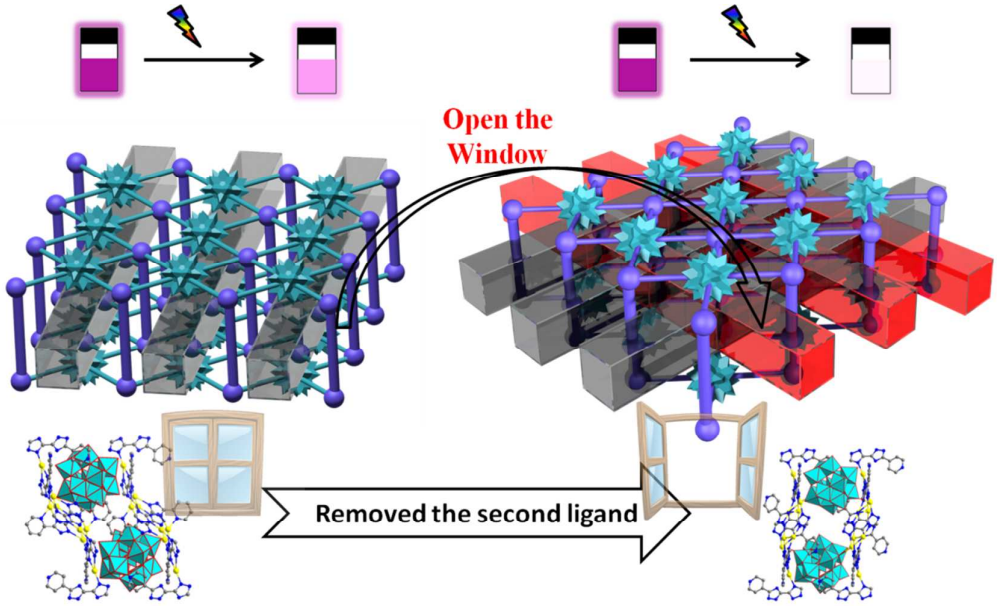


Scheme 1. Schematic representation of structure refinement and photocatalytic property of the POMCPs.

**Results and discussion**

During the rational design and synthesis of two target compounds, the most important thing is that the structure is adjusted subtly, meanwhile retaining the underlying framework. To achieve this goal, only one parameter is allowed to change in order to ensure the target compounds. In this work, we have performed many experiments *via* changing pH, temperature, and organic molecules to obtain the target compounds. When we modulated pH value, the compound crystallizes in a low value (1-3), and floccules and clear liquid were observed in other value (3.5-4.5 and 0.5-1,

respectively). When the reaction temperature is changed from 150 ℃ to 180 ℃, the compound can be obtained in the range of 170 ℃-180 ℃, and the lower the temperature is, the higher the yield is. Happily, when isomers pyttz molecules is used to adjust the structure, the aim of the work is realized. For one thing, the whole structure can be maintained through the same part of the isomers; for another, the different part of the isomers can provide a chance to refine the structure. As a result, we successfully synthesized two target compounds in the triclinic space group $P\bar{1}$ and exhibit 1D structure with similar structure but hold different tunnels. Additionally, all tungsten atoms are in +6 oxidation states, and silver atoms are in +1 oxidation states, which were confirmed by charge neutrality, coordination environments and valence sum calculations.

**Structure Description of Compound 1**

Single-crystal X-ray diffraction studies reveals that the asymmetric unit of compound **1** is constructed by four silver atoms, one pyttz-I ligand (named as L1) and two pyttz-II ligands ( named as L2-a for $H_2$pyttz-II and L2-b for Hpyttz-II ), one keggin polyoxoanion $[SiW_{12}O_{40}]^{4-}$ ($\{SiW_{12}\}$) and four crystal waters (Fig. 1a). There are four unique Ag centers: Ag1 ions are four-coordinated in a tetrahedron geometry formed by two N atoms from two pyttz ligands and two O atoms from two $SiW_{12}$ clusters; Ag2 ions are two-coordinated in a linear geometry, coordinated by two N atoms form different ligands; Ag3 and Ag4 are both three-coordinated in a triangle geometry defined by three N atoms from two L2 molecules for Ag4 and three N atoms from different pyttz ligands for Ag3. The bond distances are 2.119-2.442 Å for Ag-N and 2.513-2.595 Å for Ag-O. L1 and L2 ligands adopt two drastically different conformations, in which L1 links with three Ag centers, L2-a with one and L2-b with four. And the $\{SiW_{12}\}$ cluster provides two O atoms coordinating with Ag ions, shown in table S2.

In compound **1**, Ag centers and pyttz molecules linked each other forming the finite stick-like fragments (Fig. 1b up), which furthermore connect with zigzag-like chains (Fig. 1b down) that formed by POMs and Ag1 centers. As a result, a ladder-like organic-inorganic chain is obtained (Fig. 1c). Finally, the ladder-like chains are arranged along the *b* axis and stabilized *via* Ag4-O14 (3.074 Å) and Ag4-O24 (2.940 Å) interactions obtaining the 2D layer (Fig. 2a and S1). From the topology view, if we

assign the Ag1 centers as 5-connected nodes, $\{SiW_{12}\}$ clusters as 4-connected nodes, and the Ag-pyttz as connectors, the whole structure can be rationalized as a 4, 5-connected framework with $\{4^4;6^2\}\{4^4;6^6\}$ topology (Fig. 2b). Interestingly, the 2D layer contains quadrangular tunnels with small cavities (0.2×2.2 Å) calculated by PLATON (7.8 % of the cell volume) along *a* axis. From the structure view, there should be another tunnel along *b* axis, unfortunately, the pyridine of the pyttz-I molecule occupy the space like a closed window (Fig. 2c). And this interesting phenomenon excites us to hold a strategy to open the spaces in order to enhance the cavity of compound.

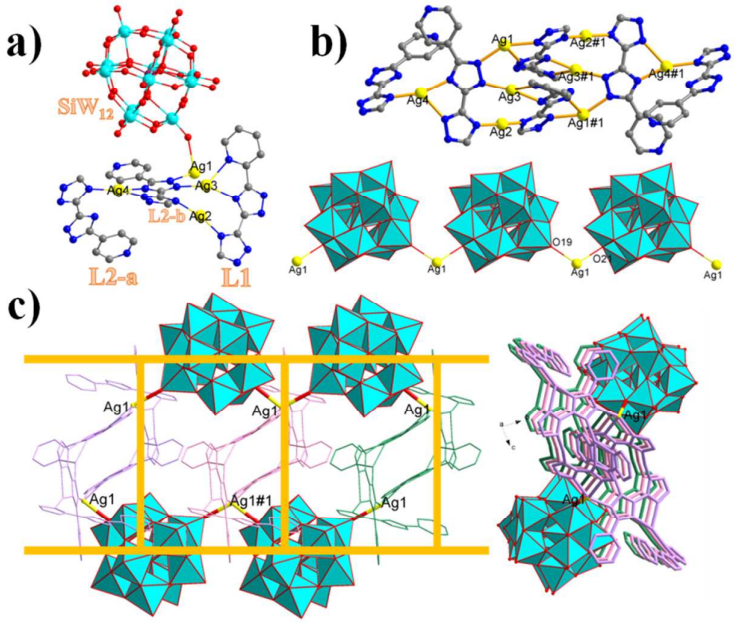


Fig.1 Combined ball/stick representation of a) the molecular structure unit of **1**, b) Sitck-like building unit and zigzag inorganic chain, c) The 1D ladder-like chain.

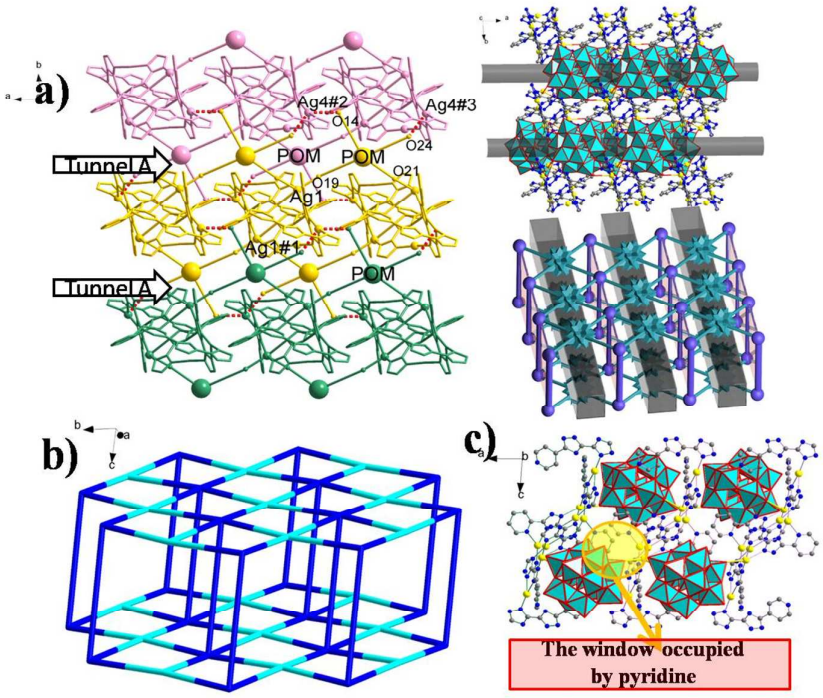


Fig. 2 a) Graphic of the 2D structure with tunnel A; b) The topology of compound **1**, c) Combined polyhedral and ball/stick representation of the closed window in 2D lay.

**Structure Description of Compound 2**

The successful isolation of compound **2** may attribute to the reasonable modulation of the coordination mode of pyttz ligand. Single-crystal X-ray diffraction studies reveals that the asymmetric unit of compound **2** is constructed by four silver atoms, three pyttz-II ligands, one $\{SiW_{12}\}$ cluster and three crystal waters (Fig. 3a). There are four crystallographically independent silver centers: Ag1 and Ag2 ions are both two-coordinated in a linear geometry, coordinated by two N atoms form different ligands; Ag3 ions are four-coordinated in a seesaw geometry formed by two N atoms from two pyttz ligands and two O atoms from two $SiW_{12}$ clusters; Ag4 are three-coordinated in a triangle geometry defined by three N atoms from two L2 molecules. The bond distances are 2.137-2.386 Å for Ag-N and 2.503-2.781 Å for Ag-O. Three crystallographically independent pyttz-II ligands adopt drastically different conformations, in which L2-a ($H_2$pyttz) links with one Ag center, and L2-b (Hpyttz) with four Ag centers and L2-c (Hpyttz) with three Ag centers. And each $\{SiW_{12}\}$ cluster provides two O atoms coordinating with Ag ions, shown in table S2.

Comparing with the structures of **1** and **2**, they have the similar structures but different spaces motifs in Scheme 1 (Tunnel A and B in **2** and only tunnel A in **1**).

More specifically, the isolated stick-like subunits formed by Ag centers and six pyttz ligands(Fig. 3b) connect with each other *via* POMs-Ag3 chains forming the ladder-like chains (Fig. 3c). As a result, compounds **1** and **2** possess the similar structure because of the similar building units (ladder-like chains). The only difference is that compound **2** contains another tunnel B due to the the structure-directing effect of pyttz-II molecules (Fig. 1c and Fig. 3c). Thus, the ladder-like chains arrange along the *b* axis forming the 2D layers containing two types of the quadrangular tunnels (Fig. 4 and Fig.S4) with large cavities (2.2×2.2 Å for both A and B) calculated by PLATON (15.1 % of the cell volume) *via* Ag4-O33 (3.119 Å) and Ag4-O5 (2.993 Å) bonds. Form the topology view, if we assign the Ag3 centers as 5-connected nodes, $\{SiW_{12}\}$ clusters as 4-connected nodes, and the Ag-pyttz as connectors, the whole structure can be rationalized as a POMCPs network with 4, 5-connected framework with $\{4^4;6^2\}\{4^4;6^6\}$ topology (Fig. 4d).

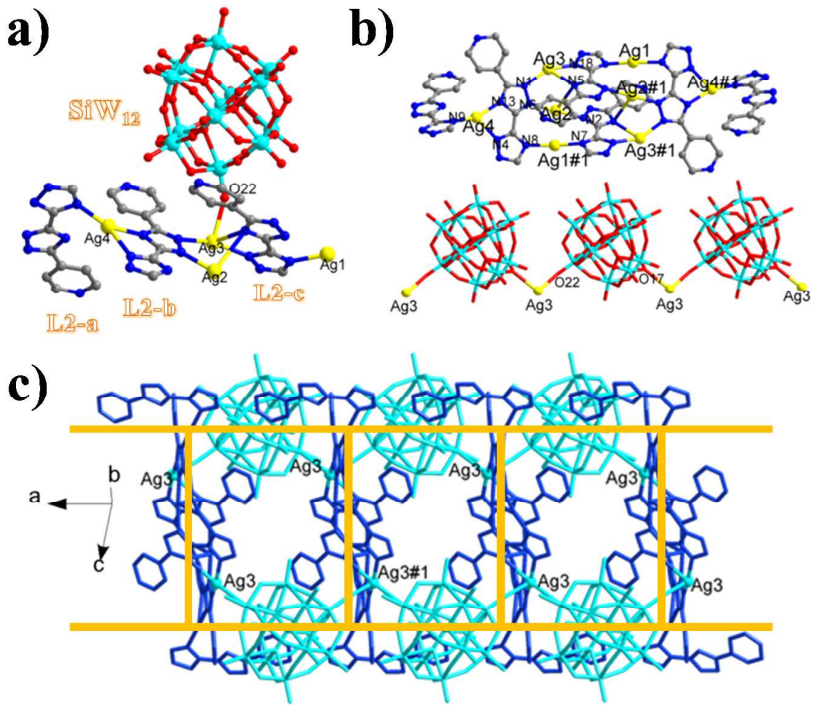


Fig. 3 Combined ball/stick representation of a) The molecular structure unit of **2**, b) Stick-like building unit and zigzag inorganic chain, c) The 1D ladder-like chain.

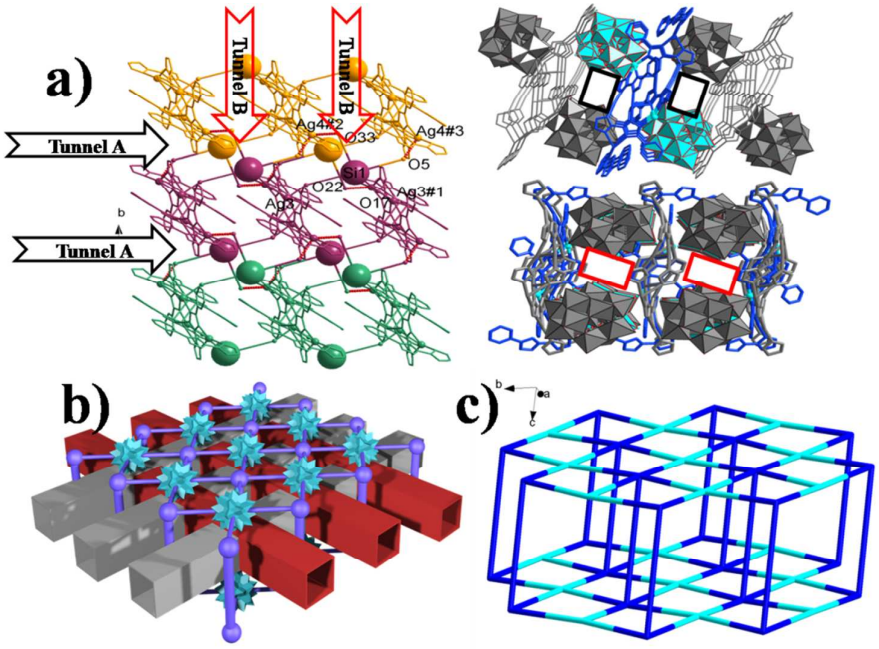


Fig. 4 a) Graphic of the 2D structure with tunnel A and B; b) Schematic of the 2D structure with two types of tunnels; c) The topology of compound **2**.

**Effect of the pyttz molecules on the structures of 1 and 2**

Unambiguously, both compounds have the similar building units, the similar stick-like units formed by the eight Ag centers and six pyttz molecules, and the similar 1D inorganic chains, but finally obtain the different motifs of tunnels (tunnel A in **1** and tunnel A&B in **2**) (Fig. S3 and S4). As shown in Fig.5, the coordination modes of pyttz molecules have high similarity in compounds **1** and **2**, so the pyttz molecule and Ag center tend to form the stick-like building. When we replace the pyttz-I with pyttz-II molecule, the main structure is not changed (namely, tunnel A is retained), but another tunnel (tunnel B) is observed, which is closed by pyttz-I molecules in **1**. This interesting phenomenon captures our attention to study the relationship between the pyttz-I molecules and the tunnels. The only difference between the two sticks is the ingredients of the center section (Fig.6). In compound **1**, the pyttz-I molecule provides a bent coordination modes to form the building units. As a results, the pyridine of the pyttz-I like a window close the space of the tunnels. When the pyttz-I is replaced with pyttz-II in compound **2**, the pyridine of pyttz-II can not coordinate with Ag ions. So the pyttz-II molecule provides a linear coordination modes to open the windows of the tunnels, which not only enhance the length of the sticks (24.200 Å in **1** and 26.521 Å in **2**), but also change the angle of the center sections (87.76 ° in **1** and 41.66 ° in **2**). The results indicate that this strategy, the

selecting isomerous pyttz molecules, is feasible for adjusting the structure of POMCPs without changing the underlying framework.

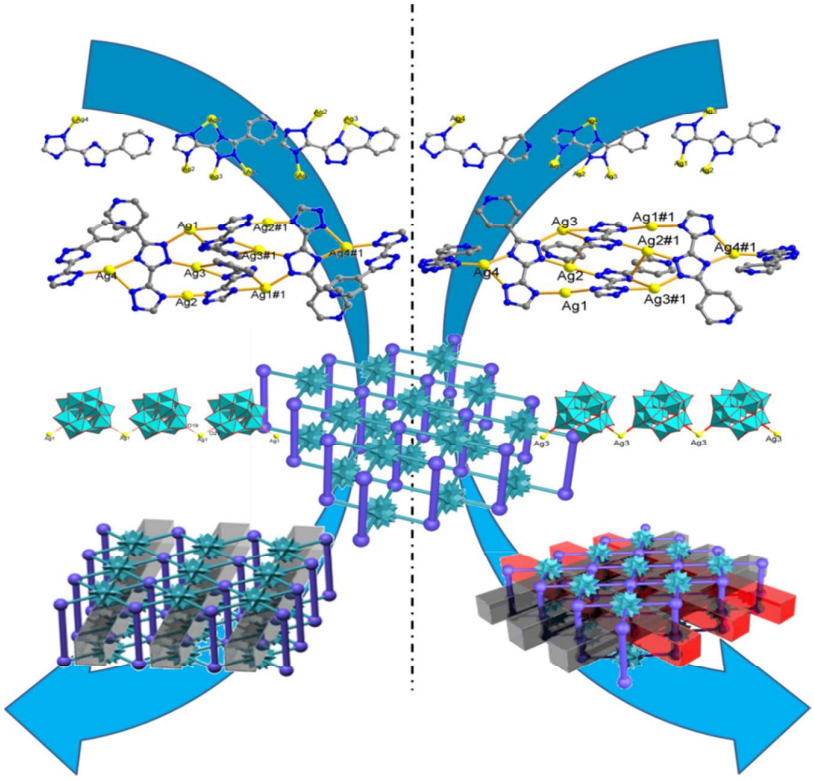


Fig. 5 Representation of the two compounds with similar underlying frameworks but different tunnels.

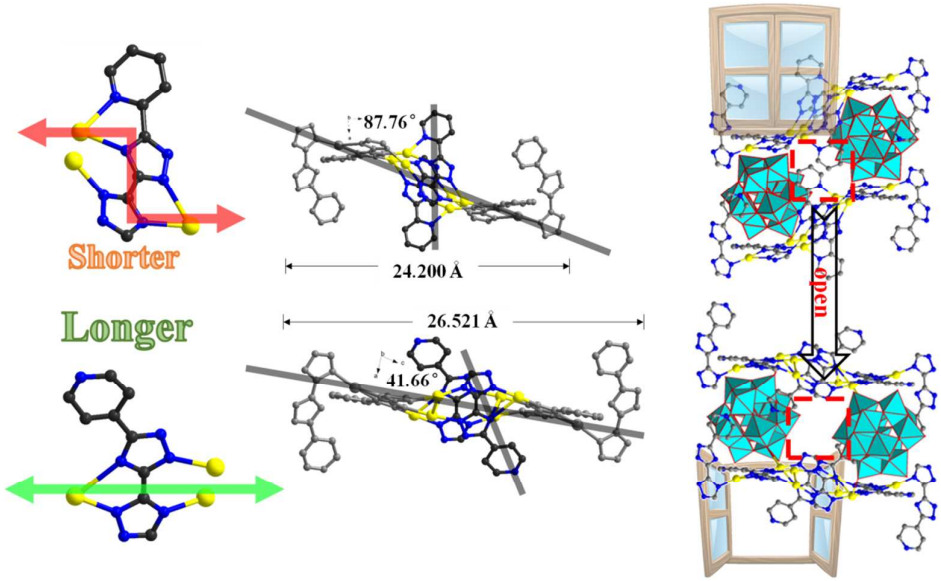


Fig. 6 Representation of the formation of tunnels A and B in compounds **1** and **2**.

**FT-IR, XRPD characterization**

The XRPD pattern for compounds **1** and **2** are presented in the Fig. S5. The diffraction peaks of both simulated and experimental patterns match well, thus indicating that the phase purity of the compound is good. Additionally, the diffraction patterns of **1** and **2** before and after use as a catalyst are identical, indicating that both compounds are stable. The difference in reflection intensities between the simulated and the experimental patterns is due to the different orientation of the crystals in the powder samples. The IR spectra of compounds are shown in Fig. S6. Characteristic bands at 972, 916 and 790 $cm^{-1}$ for **1**, 974, 910, 785$cm^{-1}$and for **2** are attributed to ν (W=O), ν (Si-O) and ν (W-O-W) vibrations, respectively. Band in the regions of 1640–1117 $cm^{-1}$ are attributed to the pyttz ligand.

**Photocatalysis properties**

The use of POMs as photocatalysts to decompose waste organic molecules so as to purify the water resources has attracted great attention in recent years. The introduction of transition-metal complexes as functional groups into POMs can enrich their potential applications. Herein, to investigate the photocatalytic activities of compounds **1** and **2** as catalysts, the photodecomposition of Rhodamine-B (RhB) is evaluated under UV light irradiation through a typical process (ESI†).

The photodegradation of RhB assisted by compounds **1** and **2** and their matrix $(NBu_4)_4[SiW_{12}O_{40}]$) are shown in Fig.7. RhB has a major absorption peak at 554nm, which decreases from 1.14 to 0.419 for **1**, from 1.10 to 0.208 for **2**, and from 1.24 to 0.540 for $(NBu_4)_4[SiW_{12}O_{40}]$. After irradiation compounds **1** and **2** for 150 min, the photocatalytic decomposition rate, defined as $1-C/C_0$, is 63.3% for **1** and 81.1% for **2**. Moreover, in contrast, the photocatalytic decomposition rate using $(NBu_4)_4[SiW_{12}O_{40}]$ as catalyst are 56.6%, respectively. The enhanced photocatalytic capability may be arisen shown in Scheme 2. Firstly, UV excitation of POMs induces a ligand to metal charge transfer (LMCT) with promoting an electron from the highest occupied molecular orbital (HOMO) to the lowest unoccupied molecular orbital (LUMO), which can be considered as a parallel process to the band-gap excitation in semiconductor photocatalyst.[15] Secondly, Ag-O clusters as bridging units facilitate the transfer of the electron from POM to POM due to the distortion of the $MO_6$ clusters, namely, Ag-pyttz may act as photosensitizer under UV light and promote the transition of electrons onto POMs. Thirdly, the POM possesses the higher charge density and exerts the considerable influence on the pseudo-liquid phase behavior of

POMs. Finally, it is more important point that the photocatalytic properties are influenced by the structure of compounds. The larger cavities in compound **2** not only increase the contact area between catalysts and crude materials but also promote more active centers to participate in the process of the reactions. As a result, the catalytic properties of compound **2** are improved. On one hand, due to non-localized electrons in POM clusters, the large numbers of the electrons delocalize in the whole spaces of the POMCPs, which plays a pivotal role on the pseudo-liquid phase behavior of POMs. On the other hand, the intermediate carbenium ions can be stabilized commendably by the higher charge density of POMs, which prove an advantage for the redox reaction of RhB.

In order to quantitatively understand the reaction kinetics for the degradation of the RhB dye by catalyst compounds **1** and **2**, we applied the pseudo-first order model[16] as expressed by eqn (1) to obtain the rate constant (κ)

$$-\ln\left(\frac{C_n}{C_0}\right) = \kappa t \qquad (1)$$

where $C_0$ is the initial concentration (0 min) of the RhB aqueous solution and $C_n$ is the concentration of the RhB aqueous solution for different times of UV illuminations, t is the time and κ is the pseudo-first order, respectively. This equation is generally used for the photocatalytic degradation process if the initial concentration of pollutant is low ($1.0\times10^{-5}$). According to eqn (1), if $[-\ln(C_n/C_0)]$ is plotted as a function of t, a straight line should be obtained whose slope is $\kappa(min^{-1})$. Fig. 7d indicates that the rate constants without catalyst for the degradation of RhB are very small, revealing that the dye practically do not degrade under UV-illumination. The rate constant values (κ) for the degradation of RhB solutions are 0.005 and 0.006 and 0.10 for their matrix and compounds **1** and **2**. And the correlation coefficient (R) also shows good statistics values of the all compounds. These results illustrate that the formation of POMCPs could improve the photocatalytic performance of the POMs.

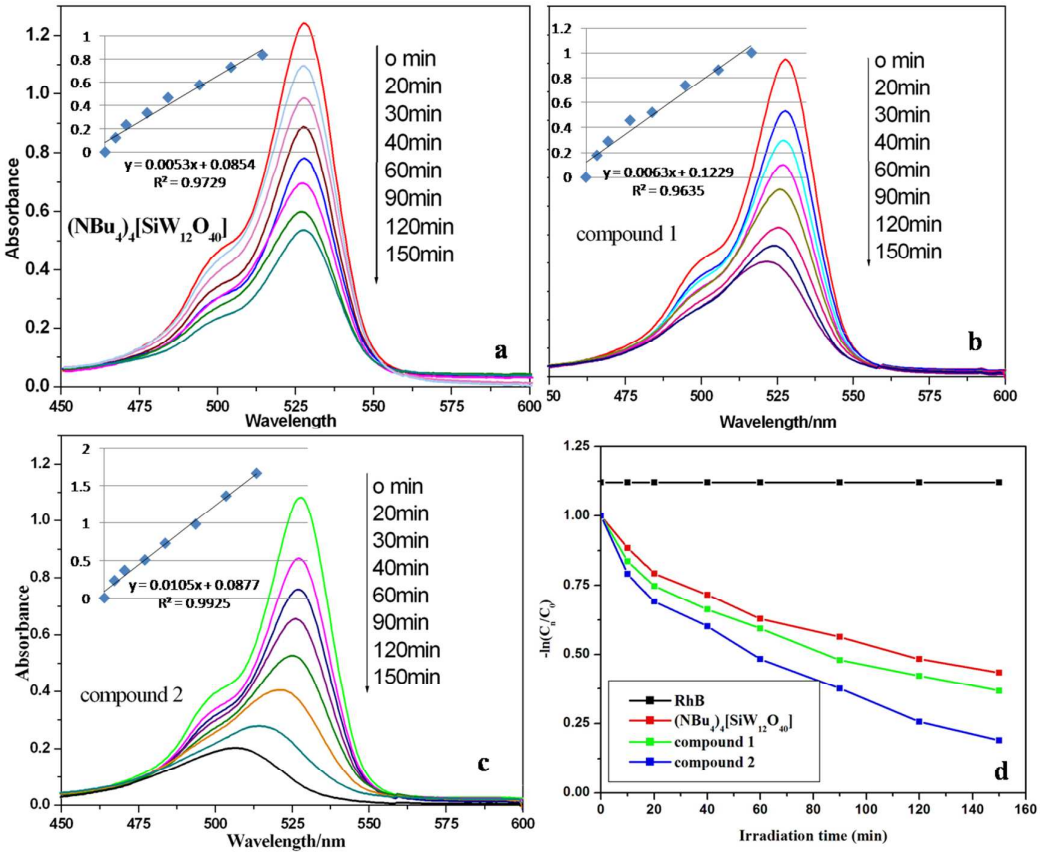


**Fig. 7** Evolution of UV-vis absorption spectra 150 min of illumination for the photodegradation of RhB by all compounds (a) $(NBu_4)_4[SiW_{12}O_{40}]$; (b) compound **1**; (c) compound **2** and (d) Kinetic of weight-based photocatalytic degradation of RhB dye by the catalysts and First-order kinetic with catalysts.

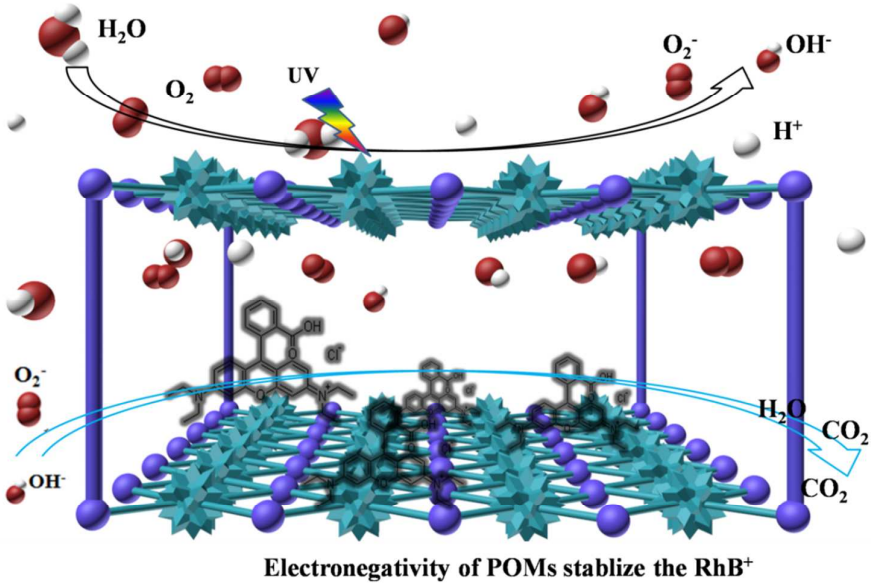


Scheme 2 Representation of the photocatalytic mechanisms.

## Experimental

**Materials and General Methods** All reagents were purchased commercially and used without further purification. The ligand ($H_2$pyttz-I and $H_2$pyttz-II) were purchased from Jinan Henghua Sci. & Tec. Co., Ltd. Elemental analyses (C, H, N and Ag) were performed on a Perkin-Elmer 2400 CHN Elemental Analyzer and on a Leaman inductively coupled plasma (ICP) spectrometer. The IR spectra were obtained on an Alpha Centaurt FT/IR spectrometer with KBr pellet in the 400-4000 $cm^{-1}$ region. The XRPD patterns were obtained with a Rigaku D/max 2500V PC diffractometer with Cu-Kα radiation, the scanning rate is 4°/s, 2θ ranging from 5-40°. UV-vis absorption spectra were recorded on a 756 CRT UV-vis spectrophotometer.

**Synthesis of $[Ag_4(H_2pyttz\text{-}I)(H_2pyttz\text{-}II)(Hpyttz\text{-}II)][HSiW_{12}O_{40}]\cdot 4H_2O$ (1).** A mixture of $H_4SiW_{12}O_{40}$ (300mg), $AgNO_3$ (150mg), $H_2$pyttz-I (30mg), $H_2$pyttz-II (60mg) and $NH_4VO_3$ (36mg) was dissolved in 12mL of distilled mater at room temperature, and stirred for 1 h in air. When the pH value of mixture was adjusted to ca.2.1 with 1M HCl, and the suspension was transferred to an 18ml Teflon-lined reactor and heated at 170 °C for 4 days. After slow cooling to room temperature, yellow block crystals were filtered, and washed with distilled water, and dried at room temperature (33% yield based on W). Elemental analysis Calcd. For $C_{27}H_{14}Ag_4N_{21}O_{44}W_{12}Si$ (4002.25): C 8.09, H 0.35, N 7.35, Ag 10.78 %; Found C 8.11, H 0.54, N 7.38, Ag 10.83 %.

**Synthesis of $[Ag_4(H_2pyttz\text{-}II)(Hpyttz\text{-}II)_2][H_2SiW_{12}O_{40}]\cdot 3H_2O$ (2).** A mixture of $H_4SiW_{12}O_{40}$ (300mg), $AgNO_3$ (150mg), $H_2$pyttz-II (90mg) and $NH_4VO_3$ (36mg) was dissolved in 12mL of distilled mater at room temperature, and stirred for 1 h in air. When the pH value of mixture was adjusted to ca.1.55 with 1M HCl, and the suspension was transferred to an 18ml Teflon-lined reactor and heated at 170 °C for 4 days. After slow cooling to room temperature, yellow block crystals were filtered, and washed with distilled water, and dried at room temperature (35% yield based on W). Elemental analysis Calcd. For $C_{27}H_{12}Ag_4N_{21}O_{43}W_{12}Si$ (3984.25): C 8.13, H 0.3, N 7.38, Ag 10.8 %; Found C 8.15, H 0.41, N 7.42, Ag 10.83 %.

***X-Ray Crystallography***

Crystal data for compounds **1** and **2** were collected on a Bruker SMART-CCD diffractometer with Mo-Kα monochromatic radiation (λ = 0.71069 Å) at 293 K. The structures were solved by the directed methods and refined by full matrix least-squares on $F^2$ using the SHELXTL crystallographic software package.[17] All the non-

hydrogen atoms were refined anisotropically. The positions of hydrogen atoms on carbon atoms were calculated theoretically. During the refinement, the command 'ISOR' was used to restrain the non-H atoms with ADP and NPD problems, which led to relative high restraint values: 200 for compound **2**. The command "ISOR" was used to refine atoms C3, C7, C8, C10, C11, C13, C14, C16, C18, C19, C23, C24, C25, C27, N5, N8, N9, N11, O1W, O6, O7, O11, O13, O17, O21 and O33 in compound **2**. Additionally, restraint command "DFIX" was introduced to restrain distances for the disordered atoms for compound **2**. It refined atoms C24 and C25, N17 and N18 in compound **2**. The positions of hydrogen atoms were calculated theoretically. The crystal data and structure refinements of compounds **1** and **2** are summarized in Table 1. Selected bond lengths and angles for compounds **1** and **2** are listed in Table S3 and S4, respectively. CCDC reference numbers 1006551 for **1** and 1006552 for **2**.

Table 1. Crystallographic and structural refinement data of **1** and **2** at 293 K.

| Compound | **1** | **2** |
|---|---|---|
| Chemical formula | $C_{27}H_{14}Ag_4N_{21}O_{44}SiW_{12}$ | $C_{27}H_{12}Ag_4N_{21}O_{43}SiW_{12}$ |
| CCDC no. | 1006551 | 1006552 |
| Formula weight | 4002.25 | 3984.25 |
| Temperature (K) | 293(2) | 293(2) |
| Wavelength (Å) | 0.71069 | 0.71069 |
| Crystal system | Monoclinic | Monoclinic |
| Space group | *P -1* | *P -1* |
| a(Å) | 11.614(5) | 11.446(5) |
| b(Å) | 12.122(5) | 12.300(5) |
| c(Å) | 23.230(5) | 25.541(5) |
| α(°) | 83.51 | 79.50 |
| β(°) | 86.40 | 78.66 |
| γ(°) | 84.97 | 87.71 |
| V(Å$^3$) / Z | 3232(2)/2 | 3466(2)/2 |
| Density (g·cm$^{-3}$) | 4.114 | 3.821 |
| Abs coeff. (mm$^{-1}$) | 22.569 | 21.043 |
| F(000) | 3532 | 3516.0 |
| Data collect θ range | 2.99-25.00 | 3.24-25.00 |
| Reflns collected | 15865 | 16334 |
| Independent reflns | 11347 | 11293 |
| Rint | 0.0374 | 0.0741 |
| Data/restraints/parameters | 11347/84/972 | 11293/200/958 |

| | | |
|---|---|---|
| Goodness-of-fit on $F^2$ | 1.076 | 1.033 |
| Final R indices [I > 2δ(I)] | $R_1$ = 0.0511,$wR_2$= 0.1106 | $R_1$ = 0.0824,$wR_2$= 0.2184 |
| R indices (all data) | $R_1$ = 0.0669,$wR_2$= 0.1205 | $R_1$ = 0.0978,$wR_2$= 0.2407 |

$R_1 = \Sigma(||F_0|-|F_c||)/\Sigma|F_0|$, $wR_2 = \Sigma w(|F_0|^2-|F_c|^2)^2/\Sigma w\,(|F_0|^2)^2]^{1/2}$

**Conclusions**

By the suitable modulating organic ligand, two new POMCPs were obtained, which possess the similar building units, the similar stick-like units and similar 1D inorganic chains, but finally form the different motifs of tunnels (tunnel A in **1** and tunnel A&B in **2**). The work indicates that this strategy, namely, selecting the isomerous pyttz molecules as reaction variation, is feasible for adjusting the structure of porous POMCPs without changing the underlying framework. This study will undoubtedly deepen our systematic understanding the assembly of POMCPs and is favor of the study about the structure-activity relationship of POMCPs. It is believed that more porous POMCPs with interesting structures as well as properties will be synthesized in the future.

**Acknowledgements**

This work is financially supported by the National Natural Science Foundation (Grant Nos. 21271089, 21072049, 21072050), the Natural Science Foundation (No.B201214) and the training program for New Century Excellent Talents in universities (1253-NCET-022) ,Postdoctoral Foundation and key program (12511z027) in Heilongjiang Province.

**AppendixA.Supplementary data**

Crystallographic data and CCDC can be obtained free of charge from the Cambridge Crystallographic Data Centre via www.ccdc.cam.ac.uk/data_request/cif. Tables of Crystal data and structure refinements and selected bond lengths (Å) , bond angles (deg) and Figures, IR, XRPD for compounds are provided in supporting information.

**References**

(1) (a) M. E. Davis, *Nature* 2002, **417**, 813; (b) F. SchOth and W. Schmidt, *Adv. Mater.* 2002, **14**, 629; (c) H. Furukawa, Kyle E. Cordova, M. O'Keeffe and O. M. Yaghi, *Science* 2013, **341**, 1230444-1.

(2) A. K. Cheetham, G. FPrey and T. Loiseau, *Angew. Chem.,* 1999, **111**, 3466; *Angew. Chem. Int. Ed.,* 1999, **38**, 3268.

(3) (a) U. Kortz, A. Muller, J. Van Slageren, J. Schnacke, N. S. Dalal and M. Dressel, *Coord. Chem. Rev.,* 2009, **253**, 2315; (c) P. Mialane, A. Dolbecq and F. Secheresse, *Chem. Commun.,* 2006, 3477; (d) P. Kogerler, B. Tsukerblat and A. Muller, *Dalton Trans.,* 2010, 39, 21; (f) Special issue on polyoxometalates: C. L. Ed. Hill, *J. Mol. Catal. A.,* 2007, **262**, 1-242.

(4) A. Dolbecq, E. Dumas, C. R. Mayer and P. Mialane, *Chem. Rev.,* 2010, **110**, 6009.

(5) (a) L. M. Rodriguez-Albelo, G. Rousseau, P. Mialane, J. Marrot, C. Mellot-Draznieks, A. R. Ruiz-Salvador, S. Li, R. Liu, G. Zhang, B. Keita and A. Dolbecq, *Dalton Trans.,* 2012, **41**, 9989; (b) F. Ma, S. X. Liu, C. Y. Sun, D. D. Liang, G. Ren, F. Wei, Y.G. Chen and Z. M. Su, *J. Am. Chem. Soc.,* 2011, **133**, 4178.

(6) (a) G. Ferey, *Chem. Soc. Rev.,* 2008, **37**, 191; (b) B. L. Chen, C. D. Liang, J.Yang, D. S. Contreras, Yvette L. Clancy, E. B. Lobkovsky, O. M. Ya ghi and S. Dai *Angew. Chem. Int. Ed.,* 2006, **45**, 1390; (c) S. Kitagawa, R. Kitaura and S. Noro, *Angew. Chem. Int. Ed.,* 2004, **43**, 2334; (d) L. J. Murray, M. Dinca and J. R. Long, *Chem. Soc. Rev.,* 2009, **38**, 1294; (e) I. Imaz, M. Rubio-Martínez, J. An, I. Solé-Font, N. L. Rosi and D. Maspoch, *Chem. Commun.,* 2011, **47**, 7287; (f) D. M. D'Alessandro, B. Smit and J. R. Long, *Angew. Chem. Int. Ed.,* 2010, **49**,6058–6082; (g) J. R. Li, R. J. Kuppler and H. C. Zhou, *Chem. Soc. Rev.,* 2009, **38**,1477; (h) R. E. Morris and P. S. Wheatley, *Angew. Chem. Int. Ed.,* 2008, **47**, 4966.

(7) (a) J. An, O. K. Farha, J. T. Hupp, E. Pohl, J. I. Yeh and N. L. Rosi, *Ncomms.,* 2012, **3**, 604; (b) X. F. Kuang, X. Y. Wu, R. M. Yu, J. P. Donahue, J. S. Huang and C. Z. Lu, *Nchem.,* 2010, **2**, 461.

(8) (a) S. C. Xiang, Z. J. Zhang, C. G. Zhao, K. L. Hong, X. B. Zhao, D. R. Ding, M, H. Xie and C. D. Wu, *Ncomms.,* 2011, **2**, 204; (b) J. Kim, B. Chen, T. M. Reineke, H. Li, M. Eddaoudi, D. B. Moler, M. O'Keeffe and O. M. Yaghi, J. *Am. Chem. Soc.*, 2001, **123**, 8239.

(9) (a) J. E. Warren, C. G. Perkins, K. E. Jelfs, P. Boldrin, P. A. Chater, G. J. Miller, T. D. Manning, M. E. Briggs, K. C. Stylianou, J. B. Claridge and M. J. Rosseinsky, *Angew. Chem. Int. Ed.,* 2014, **53**, 1; (b) S. Ma, D. Sun, M. Ambrogio, J. A. Fillinger, S. Parkin and H. C. Zhou, *J. Am. Chem. Soc.,* 2007, **129**, 1858; (c) B. Nohra, H. E. Moll, L. M. R. Albelo, P. Mialane, J. Marrot, C. Mellot-Draznieks, M. O'Keeffe, R. N. Biboum, J. Lemaire, B. Keita, L. Nadjo and A. Dolbecq, *J.*

*Am. Chem. Soc.,* 2011, **133**, 13363; (d) Q. Yang, X. Chen, Z. Chen, Y. Hao, Y. Li, Q. Lu and H. Zheng, *Chem. Commun.,* 2012, 48, 10016.

(10) P. Falcaro, A. J. Hill, K. M. Nairn, J. Jasieniak, J. I. mardel, T. J. Bastow, S. C. Mayo, M. Gimona, D. Gomez, H. J. Whitfield, R. Riccò, A. Patelli, B. Marmiroli, H. Amenitsch, T. Colson, L. Villanova and D. Buso, *Ncomms.,* 2011, **2**, 237.

(11) S. T. Zheng, T. Wu, F. Zuo, C. Chou, P. Feng and X. Bu, *J. Am. Chem. Soc.*, 2012, **134**, 1934.

(12) (a) W.G. Klemperer, T. A. Marquart and O. M. Yagi, *Angew. Chem., Int. Ed.,* 1992, **31**, 49; (b) W. G. Klemperer, T. A. Marquart and O. M. Yagi, *Angew. Chem.,* 1992, **104**, 51; (c) V. W. Day, W. G. Klemperer and O.Yagi, M. *J. Am. Chem. Soc.*, 1989, **111**, 5959; (d) G. K. Johnson and E. O. Schlemper, *J. Am. Chem. Soc.*, 1978, **100**, 3645; (e) L. Chen, F. L. Jiang, Z. Z. Lin, Y. F. Zhou, C. Y. Yue and M. C. Hong, *J. Am. Chem. Soc.,* 2005, **127**, 8588; (f) M. I. Khan and J. Zubieta, *Angew. Chem., Int. Ed.*, 1994, **33**, 760.

(13) (a) J. Q. Sha, M. T. Li, J. W. Sun, P. F.Yan, G. M. Li and L. Zhang, *Chem. Asian J.* 2013, **8**, 2254; (b) J. Q. Sha, J. W. Sun, C.Wang, G. M Li, P. F.Yan and M. T. Li, *Cryst. Growth Des.,* 2012, **12**, 2242; (c) J. Q. Sha, J. W. Sun, M.T. Li,; C. Wang, G.M. Li, P.F.Yan and L. J. Sun, *Dalton Trans.*, 2013, **42**, 1667.

(14) M. T. Li, J. Q. Sha, X. M. Zong, J. W. Sun, P. F.Yan, L. Li and X. N. Yang, *Cryst. Growth Des.,* 2014, **14**, 2794.

(15) S. Kim, H. Park and W. Choi, *J. Phys. Chem. B, 2*004, **108**, 6402.

(16) A. R. Malagutti, H.A. J. L. Mourao, J. R. Garbin and C. Ribeiro, *Appl. Catal. B.,* 2009, **90**, 205.

(17) (a) G. M. Sheldrick, SHELXS-97, Program for Crystal Structure Solution; University of Göttingen, Germany, 1997; (b) G.M. Sheldrick, SHELXL-97, Program for Crystal Structure Refinement; University of Göttingen: Germany, 1997.

# Structure Refinement and Photocatalytic Properties of Porous POMCPs by Selecting the Isomerous PYTTZ

Liang Li [a,b], Jing-Wen Sun[a], Jing-Quan Sha[a* b], Guang-Ming Li[a], Peng-Fei Yan[a*], Cheng Wang[a], Lian Yu [b]

[a]*Key Laboratory of Functional Inorganic Material Chemistry (MOE), P. R. China; School of Chemistry and Materials Science, Heilongjiang University; Harbin 150080, P. R. China*

[b]*The Key Laboratory of Biological Medicine Formulation，Heilongjiang Provincial; School of Pharmacy, Jiamusi University, Jiamusi, 154007, PR China*

Two POMCPs with similar building units and different motifs of tunnels were reported.